12

Features of the application of the virial theorem for magnetic systems with quasi-force-free windings

© *G.A. Shneerson,*[1] *S.L. Shishigin*[2]

[1] Peter the Great Saint-Petersburg Polytechnic University,
195251 St. Petersburg, Russia
[2] Vologda State University,
160000 Vologda, Russia
e-mail: gashneerson@mail.ru, ctod28@yanex.ru

The article shows that in a magnetic system with a thin-walled balanced winding close to a force-free one, a significant increase in the parameter $\theta = W_M \gamma / M \sigma_M$, is possible, which, according to the virial theorem, characterizes the ratio of the energy of the magnetic system W_M to the weight of equipment with a material density γ, where under the action of electromagnetic forces there appears a mechanical stress σ_M. In a quasi-force-free magnetic system, the main part of the winding is in a state of local equilibrium, and only a relatively small part of the equipment is subject to stress. This part determines the weight of the entire system, and this weight can be minimized. The configurations of balanced thin-walled windings are developed, at the boundaries two boundary conditions are fulfilled simultaneously — the absence of the induction component normal to the boundary and the constancy of the product of induction and radius. The authors consider an example of a system consisting of a main part - a sequence of balanced „transverse" modules in the form of flat discs and end parts, consisting of a combination of „transverse" modules and „longitudinal" ones, having the form of rings elongated along the axis with balanced end parts. It is shown that in the system under consideration, the characteristic dimensionless parameter θ with an unlimited increase in the number of elements of the main part can reach a value of about 24, and when the number of these elements changes within $20-40$, it changes from 6 to 9.

Keywords: Quasi-force-free magnetic field, field energy, mass of a magnetic system, virial theorem, minimization of the ratio of mass to energy.

DOI: 10.21883/TP.2022.02.53577.249-21

Introduction

The bulk force, equal to the sum of the electromagnetic force and divergence of the elastic stress tensor, is zero in a magnetic system being in equilibrium. The calculations given in papers [1–3] provide the following expression that relates magnetic system field energy W_M to the integral of elastic stress tensor S_{ii} (virial theorem):

$$W_M = \int \frac{B^2}{2\mu_0}\, dV = -\int_V S_{ii}\, dV. \qquad (1)$$

The first integral here is taken for the whole unlimited region. The second one covers region V where the components of the elastic stress tensor are different from zero. Magnetic system cross-section and, consequently, volume and mass are determined by the level of permissible mechanical stresses in magnetic system elements loaded by electromagnetic forces.

Equation (1) is used in the Longmire's book [2] and in other papers for estimating the magnetic system's energy to mass ratio. Such estimates in the simplest case are based on the assumption that a load caused by electromagnetic forces is perceived only by current-carrying conductors that generate the field. If the material of all conductors in this case has identical density γ, the ratio of magnetic field energy to winding mass $M = \gamma V$ follows from the given equality (1):

$$\frac{W}{M} = \theta \frac{\sigma}{\gamma}, \qquad (2)$$

where σ — quantity characterizing the stressed state of the winding material, θ — typical dimensionless parameter (virial coefficient).

The energy to mass ratio in particular systems is calculated taking into account their design features. For instance, calculations of a torque-free thin-walled winding, where the value of the tangential stress component was used as σ, yield the value $\theta = 0.61$ [4]. The generally held opinion is that virial coefficient θ does not exceed the unity. This assumption in general terms is given in book [2]. It was confirmed by calculations of particular systems in [5–7] and the data given in the ample survey [8]. Japanese researchers [9–12] have demonstrated that integral equilibrium in the axial or radial direction can be achieved by placing the conductors at a certain angle on a toroidal surface. Local equilibrium is not present in the considered systems, the load is perceived by conductors, and virial parameter θ is close to unity.

Magnetic system mass in the general case is determined both by current-carrying conductors and by other structural elements that ensure its strength, e.g. reinforcements. Several recent papers have studied the possibilities of constructing locally balanced (quasi-force-free) thin-walled windings. A survey of these papers is given in book [13]. The application of such windings makes it possible to construct magnetic systems with a decreased mass of loaded elements. A strictly force-free system is perfect. However, it was demonstrated in [2,3] that a magnetic system of finite dimensions with a force-free system shall have boundaries exposed to electromagnetic forces. Therefore, the task of increasing the energy to mass ratio in systems with quasi-force-free windings comprises two parts. The first one is creation of a magnetic system as close as possible to the force-free one. The second one is minimization of the mass of elements that remain loaded by electromagnetic forces. The goal of this paper is show possible ways to construct magnetic systems with quasi-force-free windings that allow for increasing the energy to mass ratio of a magnetic field and achieving values of virial coefficient θ much larger than unity.

1. Background. Problem of minimization of mass of the magnetic system's unbalanced part

Thin-walled quasi-force-free windings in the local equilibrium state, when absolute values of magnetic field density take on equal values $B = |\mathbf{B}|$ on both winding sides, are close to strictly force-free windings. Residual equivalent stress in such a winding, calculated using the Mises formula, is characterized by value $\sigma_M = \eta B^2/(2\mu_0)$. Strength coefficient η in a locally balanced thin-walled winding can take on a value much smaller than unity. Threat, number η does not depend on winding thickness Δ, but is determined by ratio Δ/R, where R is curvature radius of the surface where the winding is located. In particular, we have $\eta \approx 0.2$ [14] in a single-layer cylindrical winding on condition of $\Delta/R \approx 0.1$. Cross-section and, consequently, mass of balanced conductors in a locally balanced winding is determined not by material strength, but by other factors, e.g., by critical current density. A limit case in this paper will be a system with a quasi-force-free winding where the conductor thickness is so small that mass of such a winding can be neglected as compared to mass of the system elements exposed to electromagnetic forces.

An example of an axially symmetrical magnetic system with a partially balanced boundary is the configuration in Fig. 1 in the form of a module extended along the axis („longitudinal"), in the shape of a cylinder with inner radius R_1 and outer radius R_2 with a thin winding placed thereon [13]. The azimuthal component of the electromagnetic force must be equal to zero at its whole boundary, consequently, the normal component of poloidal field density must be absent. This is true if the condition is
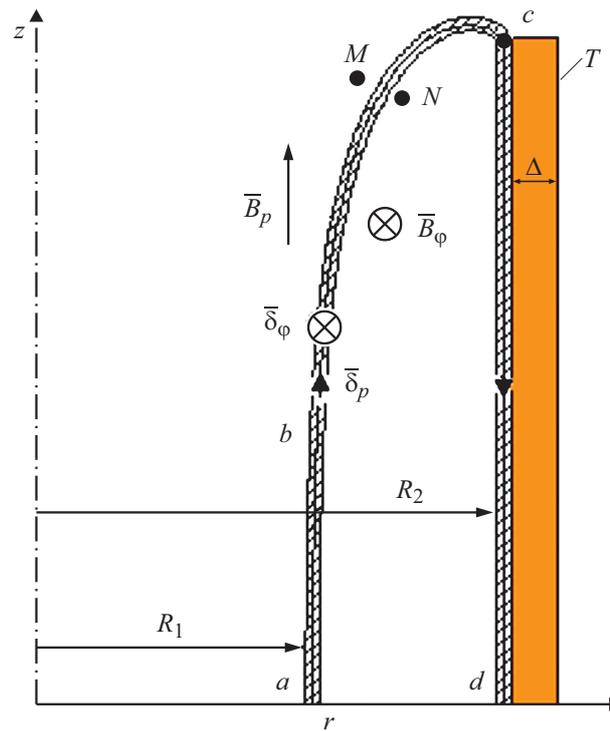
Figure 1. Semi-infinite partially balanced thin-walled winding with external reinforcement T.

met

$$\psi_P = rA_\phi = \text{const} = C_1, \quad (3)$$

where ψ_P — flux function of poloidal field, A_φ — azimuth component of vector potential. Absolute values of poloidal field density on the balanced part of the thin-walled boundary abc (Fig. 1) at point M and azimuthal field density at point N must be equal to

$$B_P(M) = B_P(N) = \mu_0|i_P|/(2\pi r) = \mu_0|\psi_i|/r, \quad (4)$$

where i_P — poloidal current in the winding, $\psi_i = \mu_0 i_P/2\pi$ — poloidal current function, r — radial coordinate of point N. Thus, the second boundary condition shall be met at this area:

$$rB_P = \mu_0|\psi_i| = \text{const} = C_2. \quad (5)$$

Plotting of a field with the above-mentioned two boundary conditions is an example of a nonlinear problem, since a boundary shape is not assigned but is generated during solving. Similar problems are considered in electrostatics, in the theory of perfect liquid jets. Their difference consists in the fact that values of the rB_p product are constant in the considered problem on the computational region boundaries, while constancy of electric field intensity on a part of the boundary is assigned in electrostatics problems, and constancy of flow velocity — in the theory of jets. Many papers and several monographs, e.g. [15–19], are dedicated to describing free-boundary flows in hydromechanics and construction of electrodes with a constant field intensity in
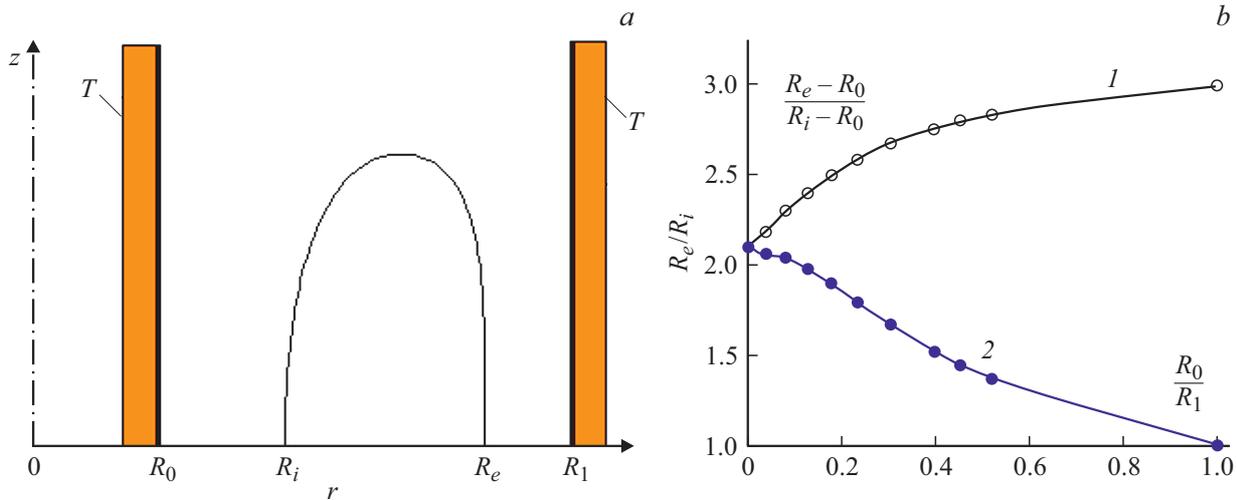
Figure 2. *a* — fully balanced thin-walled winding of great length (longitudinal module), located in the gap between two coaxial shields; *b* — dependences characterizing the parameters of the longitudinal balanced module located between two coaxial shields: *1* — $(R_e-R_0)/(R_i-R_0) = f(R_0/R_1)$, *2* — $R_e/R_i = f(R_0/R_1)$.

electrostatics. The conformal mapping method is efficiently used in solving such plane field problems. Results of such calculations can be used in calculations of axisymmetrical systems with force-free windings at boundary areas located away from the axis, where the field is close to a plane one.

The method described in [19] was used in this paper to construct winding configurations meeting the specified conditions. The procedure for constructing free-boundary shapes by the iteration method is briefly described in the Appendix.

The example in Fig. 1 demonstrates the aforesaid typical feature of magnetic systems with a force-free field: such a system cannot be completely force-free [2,3]. In particular, analytical solutions of plane problems show that in the general case both boundary conditions can occur only on a part of the boundary. For instance, electric field intensity can be constant on the area in the vicinity of the electrode edge [16,17]. A shape on whose boundary both conditions are met can be constructed only in a few cases. An additional factor in axially symmetrical two-dimensional configurations is a different law of intensity decrease of the poloidal and azimuthal fields in case of radius increase: $1/r^2$ in the first case and $1/r$ in the second case.

Boundary formation by the iteration method has shown that the shape with a balanced area shown in Fig. 1 can be constructed if the ratio of outer radius R_2 to inner radius R_1 does not exceed the value $A = R_2/R_1 \sim 1.64$. For a long magnetic length system we have the following expression for the total energy of poloidal and azimuthal fields per unit length: $W_M' \sim \pi R_1^2 (1/2 + \ln A) B_0^2/\mu_0$, where B_0 is density of a homogeneous poloidal field on the axis of a long magnet. The balanced boundary *abc*, which comprises a part of the internal cylindrical boundary and its end area, adjoins the unbalanced outer cylindrical part of winding *cd*, where the condition of constancy of functions ψ_P and ψ_i

is met, but condition (4) is not met. Neglecting the magnetic pressure of a poloidal field, we can assume that the unbalanced part of the winding is exposed to magnetic pressure $P_M = (1/2\mu_0)B_\varphi^2$ where $B_\phi = B_0/A$ is azimuthal field density. Cylindrical reinforcement T is required for holding this winding part (Fig. 1). The action of magnetic pressure in a thin reinforcement with thickness $\Delta \ll R_2$, which holds the thin winding, gives rise to azimuthal mechanical stress $\sigma_M \approx \sigma_\phi = P_M R_2/\Delta$. From here we find the reinforcement thickness and mass (per unit length) $\Delta_r = P_M R_2/\sigma_M$, $M' = 2\pi R_2\Delta\gamma = 2\pi R_2^2 P_M\gamma/\sigma_M$. Then we find the energy to mass ratio

$$\frac{W_M'}{M'} \approx \frac{\sigma_M}{\gamma}\left(\frac{1}{2} + \ln A\right). \qquad (6)$$

According to formula (2), the virial coefficient takes on value $\theta = \gamma W_M'/\sigma_M M' \sim 1/2 + \ln A$. The limit value of this parameter for the system shown in Fig. 1 is $\theta \sim 0.5 + \ln 1.64 \sim 1$.

Book [14] gives the results of configuration calculations for a semi-infinite module located in the gap between two coaxial cylinders with radii R_0 and R_1 with a zero magnetic potential specified on them (Fig. 2, *a*). The calculations by the iteration method (Appendix) showed that at the specified value of R_1/R_0 ratio there is only one shape having inner radius R_i and outer radius R_e, on the whole boundary of which the rA_φ and rB_p products are maintained constant. Fig. 2, *b* shows the dependences of the $(R_1-R_0)/(R_i-R_0)$ ratio and the $A=R_e/R_i$ aspect ratio on parameter R_0/R_1. In the limit case $R_0/R_1 = 0$, when the balanced winding is in a coaxial cylindrical shield, the said boundary conditions can be met on the entire boundary only in case of a certain radius ratio: $R_i/R_e/R_2 \sim 1/2.12/2.57$ [14]. Thereat, $R_1^2 = R_e^2 + R_i R_e$. Magnetic field energy of this system per unit length is $W_M' = \pi R_0^2[1 + 1/A + 2\ln A]B_0^2/2\mu_0$. The

unbalanced element in this system is the short-circuited diamagnetic shield.[1] It is exposed to magnetic pressure of a poloidal field with density $B(R_1) = R_0 R_i / R_e$. Mass of the thin-walled external reinforcement that perceives the magnetic pressure onto the shield is $M' = \pi R_i^2 (1 + 1/A)(B_0^2/\mu_0)/(\gamma/\sigma_M)$. Parameter θ is determined using the formula

$$\theta = \frac{1 + 1/A + 2\ln A}{2(1 + 1/A)} \sim 1, \qquad (7)$$

where $A \sim 2.12$. As in the previous example, $\theta \sim 1$. In the limit case, when condition $R_1 - R_0 \ll R_0$ is met, and the field in the gap is close to a plane one, the following ratios hold true to the equilibrium configurations in Fig. 2: $R_i - R_0 = R_1 - R_e = (R_1 - R_0)/4$, $(R_1 - R_0) = 2(R_e - R_1)$.

A configuration of current lines on the modules' boundaries can be calculated within the framework of the model of the thin-walled force-free winding. It has been shown in [20] that, when the value of the ratio of azimuthal and poloidal field densities on both winding sides are known, current lines are described by an equation that relates the increment of the azimuthal coordinates of a point on a current line upon a change in its radial coordinate from value r_1 to value r_2 and an offset by segment dl_p in plane $r-z$:

$$\Delta\varphi = \int_{r_1}^{r_2} \frac{B_p dl_p}{B_\varphi r}. \qquad (8)$$

On the balanced areas, the angle between the vector of linear current density and a tangent line to the outline of the thin winding's longitudinal cross-section at each point is $45°$. In this case the vector of linear current density is parallel to the sum of poloidal and azimuthal field density vectors which are equal in magnitude. Formula (8) in this case is as follows

$$\Delta\varphi = \int_{r_1}^{r_2} \frac{dl_p}{r}. \qquad (9)$$

Current lines on straight-line segments of equilibrium boundaries of the longitudinal module with radius R have a spiral shape: $\Delta z = R\Delta\varphi$. Boundaries $dl_p = dr$ and current lines on the plane part are described by the logarithmic spiral equation

$$\Delta\varphi = \int_{r_1}^{r_2} \frac{dr}{r} = \ln\frac{r_2}{r_1}. \qquad (10)$$

An unbalanced system element in the form of a cylinder (reinforcement or shield) is present in all the considered examples with longitudinal modules. Length of such a cylinder is little different from length of a balanced module. Therefore, virial parameter θ in such systems is close to unity. A drastic way to increase this parameter is an abrupt reduction of the mass of the elements perceiving the unbalanced radial force. This requires a reduction of the length of these elements and the forces acting on them.

2. Energy to mass ratio in a system of balanced transverse modules

An abrupt decrease of the mass of unbalanced elements is possible in a magnetic system consisting of a set of alternating transverse modules. Two variants of this system are shown in Fig. 3 and 4. Each transverse module is a thin-walled locally balanced winding having the shape of a rotation body whose axial size is much smaller than the outer radius. In a system of unlimited length they form a periodic structure with pitch h. A real finite-length system, in addition to a set of alternating transverse module, comprises two end parts of the magnetic system. Section 3 shows that these parts can be constructed so that the boundary conditions in a system with a finite number of transverse modules remain the same as in a system of unlimited length. According to boundary condition (2), the flux function of the poloidal field on the surface of each module takes on a constant value which is equal in absolute magnitude for each modules and changes its sign upon transition from each module to the next one. Thereat, condition $\psi_P = 0$ is met on the planes being the boundaries of system elements. Then we will consider the configurations where the pitch of the system of plane modules is several times smaller than their outer radius. Therefore, the form of equilibrium shapes in the vicinity of the inner radius is determined by choosing a R_0/h ratio, where h is the system pitch (Fig. 3). The modules of two types shown in Fig. 3, 4 differ only in the configurations of the right-hand parts located away from the axis. Azimuthal and poloidal field densities on the edge (nearest to the axis) of each of these modules at point C $(r = R_0)$ take on absolute values $B(C) = \mu_0|i|2\pi R_0 = \mu_0|\psi_i|/R_0$, while at the other points of the balanced part of the boundary we have the following according to condition (3)

$$B_p = B_\varphi = G_0/r, \qquad (11)$$

where $G_0 = B(C)R_0$. Taking a randomly selected value of the flux function at the module boundary $|\psi_P| = \psi_0$, we must calculate the configuration of a module on a part of whose boundary the constancy of the $rB = G_0$ product is maintained. As distance from the axis increases, the module becomes a flat disk having thickness t_0, separated by gaps $d_0 = (h - t_0)$ from the adjacent modules. This ratio takes on value $t_0/h = 1/2$ in the limit case of a plane field, when condition $R_0/h \gg 1$ is met. Dependence $B_p = 2\psi_0/rd_0$ occurs in the middle of the transverse module's boundary, away from its edge, so that:

$$G_0 = 2\psi_0/d_0. \qquad (12)$$
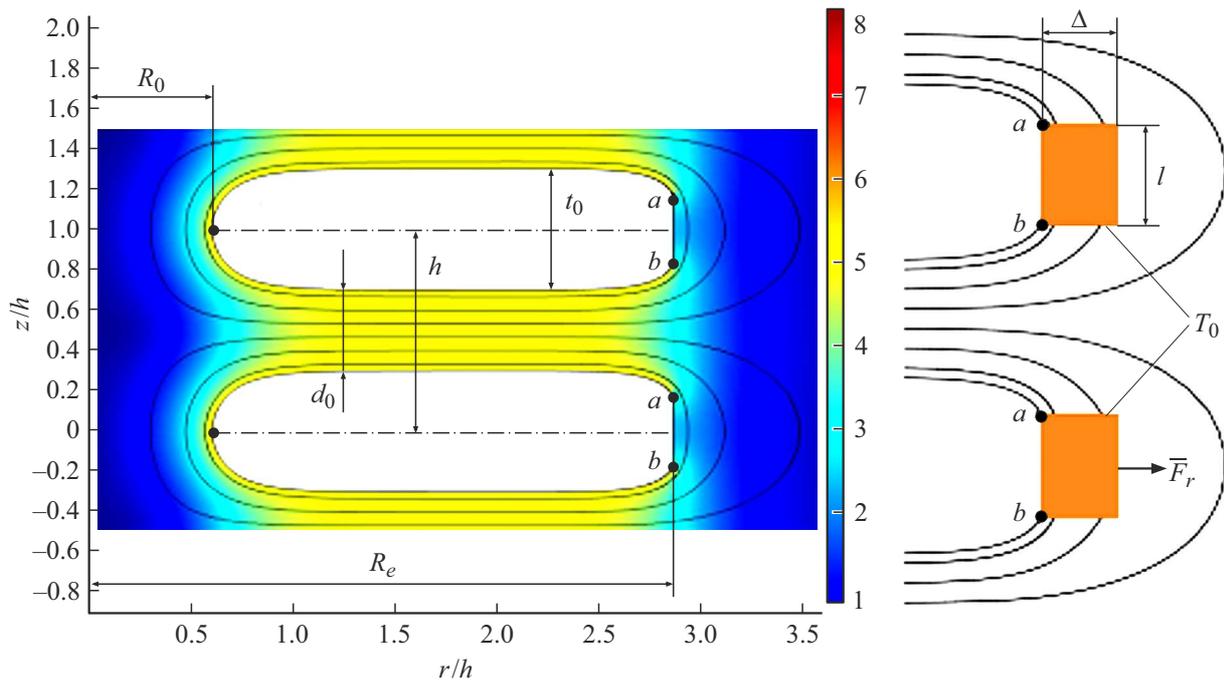
Figure 3. Two elements of a sequence of transverse modules (having unlimited length) with a partially balanced thin-walled winding and reinforcement T_0. Values of dimensionless quantity Brh/ψ_0 are plotted on the color scale.
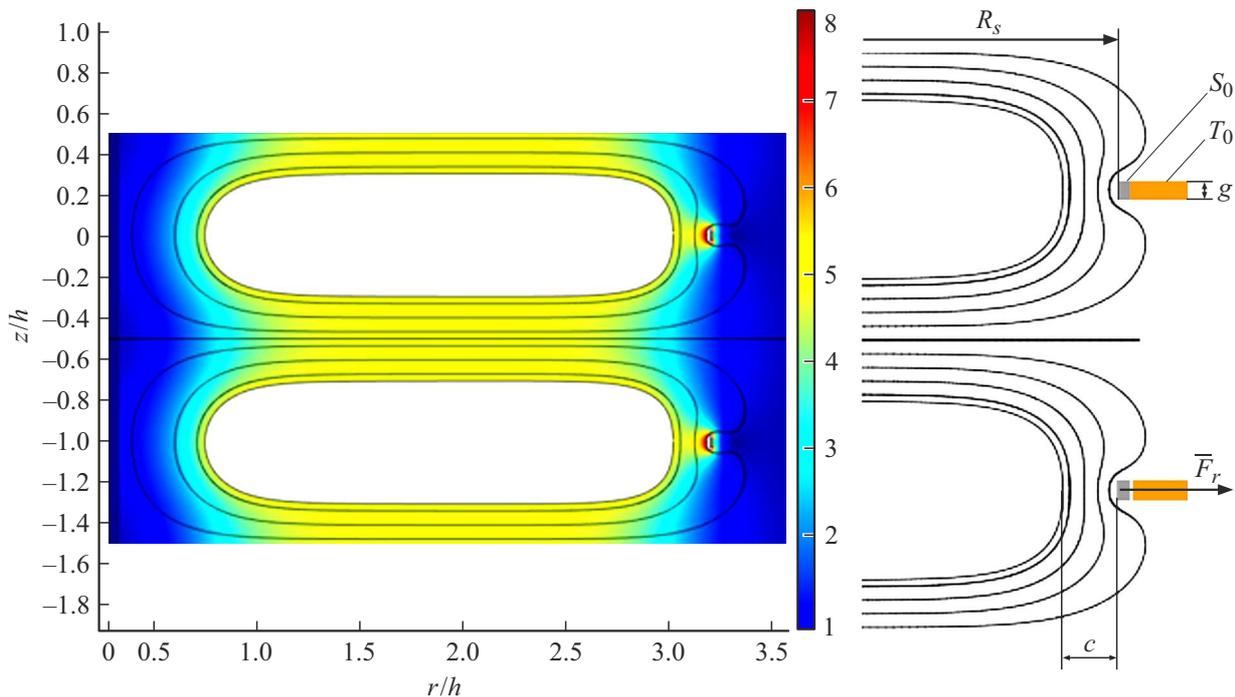
Figure 4. Two elements of a sequence of transverse modules (having unlimited length) with a fully balanced thin-walled winding, short-circuited ring (ring) S_0 and reinforcement T_0.

Fig. 3 shows the modules of the first type where the local equilibrium condition is met on the boundary except a ring-shaped area having width $l = ab$ with radius R_e. The equilibrium conditions on this area are not met, magnetic pressure of the azimuthal field is higher than that of the poloidal one, and a dielectric reinforcement with thickness Δ is required to hold the winding. Relative sizes being unchanged, the whole magnetic system under consideration (including the set of transverse modules and the end parts) is characterized by two initial parameters: flux function ψ_0

and pitch h. Magnetic field energy of one module W_1 can be calculated with a certain error (disregarding the edge effects) using a formula based on the assumption that a change in poloidal and azimuthal field densities in region $R_0 < r < R_e$ corresponds to dependence (11):

$$W_1 = \int_{R_0}^{R_e} \frac{G_0^2 \pi h r dr}{\mu_0 r^2} = W_0 \left(\frac{h}{d_0}\right)^2 \ln \frac{R_e}{R_0}, \qquad (13)$$

where $W_0 = (4\pi\psi_0^2)/(\mu_0 h) = 10^7 \psi_0^2/h$ is the typical energy of the magnetic system.

The exact energy value can be conveniently presented as $W_1 = \lambda W_0 (h/d_0)^2 \ln(R_e/R_0)$. Correction factor λ close to unity can be found by a numerical calculation of the field. Magnetic pressure of an azimuthal field with density $B(R_e) = G_0/R_e$ on an unbalanced area of the boundary in the form of a ring with width l and length $2\pi R_e$ gives rise to radial force $\mathbf{F}_r$. Neglecting the action of a weaker poloidal field on this area, we can calculate the absolute value of force per unit length of the ring, while assuming that azimuthal field density decreases according to (11):

$$F' = F_r/2\pi R_e = QlB^2(C)R_0^2/2\mu_0 R_e^2 = 2Q \frac{\psi_0^2 l}{\mu_0 d_0^2 R_e^2}. \quad (14)$$

Q in this formula is a dimensionless factor determined by relative dimensions of the magnetic system. Reinforcement T_0 (Fig. 3) with cross-sectional area S must be used to hold the winding with an unbalanced boundary area. Stress $\sigma_\varphi \approx F'R_e/S$ occurs in the reinforcement when $R_e \gg S^{1/2}$. In the case under consideration it is close to equivalent stress σ_M calculated using the von Mises formula. Then we calculate the mass of the reinforcement made of a material having the specified mechanical stress σ_M

$$M_1 = 2\pi\gamma R_e S = \frac{2\pi\gamma R_e^2}{\sigma_M} = M_0 Q \left(\frac{h}{d_0}\right)^2 \left(\frac{l}{h}\right), \qquad (15)$$

where γ is reinforcement material density, $M_0 = (4\pi\psi_0^2/\mu_0 h)(\gamma/\sigma_M)$ is typical mass of the magnetic system. Mass of a reinforcement in case of the specified length of area l, which receives magnetic pressure, does not depend on radius R_e and its cross-section area similarly to an identical example given in Longmire's book [2]. Formulas (12), (14) are used to find an approximate value of the virial coefficient of the transverse module

$$\theta_1 = \frac{W_1 \gamma_1}{M_1 \sigma_M} = \Lambda \ln \frac{R_e}{R_0}. \qquad (16)$$

Dimensionless parameter $\Lambda = \lambda h/lQ$ in a system of the first type (Fig. 3) is determined by system's relative sizes characterized by parameter R_0/h. Adopting $\lambda = 1$ and $Q = 1$, we find an estimated value of number $\Lambda = h/l$.

The configuration of the equilibrium shape is formed during a numerical calculation. Parameters ψ_0 and h drop out of from the formula for the energy to mass ratio.

Therefore, they can be chosen at random during a numerical calculation. In the considered examples they were taken equal to unity. It should be noted that as the R_0/h ratio increases, the equilibrium shape becomes all the closer to the one calculated for a plane field. Thickness of this shape t_0 is equal to half the pitch h, while length l of the unbalanced area is equal to zero [16,17]. Thus, when the said ratio increases, reinforcement mass becomes arbitrarily small, while coefficient θ_1, calculated for an element of an unlimited-length system, can be arbitrarily large. This assumption becomes void for systems with an unlimited number of elements, for which mass in the limiting case is determined by the end parts of the magnetic system.

Construction of equilibrium shapes by the iteration method, described in the Appendix, makes it possible to meet both conditions on the module's external boundary with an acceptable accuracy. This is confirmed by an example of a module of the first type given in Fig. 3. The ratio of equilibrium shape's radii for the chosen value $R_0/h = 0.75$ is $R_e/R_0 = 2.86$. Condition $B_p r = 4.2\psi_0/h$ is met on the balanced area of the boundary with an error less than 3%. Construction can be more precise, but it little affects the results of calculation of magnetic field energy and mass of the short-circuited conductor that perceives the load. The calculation has made it possible to find module thickness t_0, half the inter-module gap $d_0 = h - t_0$, length of balanced area l, flux density at point C. The values of the corresponding dimensionless parameters are: $d_0/h = 0.42$, $t_0/h = 0.58$, $l/h = 0$, $B(C) = 6.35\psi_0/h^2$. Thereat, the estimated value of parameter $T = h/l = 2.94$. It corresponds to the virial parameter value $\theta_1 \sim 8.4$. A field and force calculation using the Comsol Multiphysics program allows for determination of the numerical values of dimensionless energy and mass of one module of the first type: $W_1 \sim 5W_0$, $M_1 \sim 0.62M_0$, which yields a close value of the virial coefficient: $\theta_1 \sim 8.06$.

The second type of equilibrium shapes occurs when a quasi-force-free winding with outer radius R_e is in the field of a coaxial short-circuited loop (diamagnetic shield). Such a loop can be, for instance, a thin ring of rectangular cross-section S_0 with reinforcement T_0 (Fig. 4). In this case the winding is fully balanced, a load is perceived by the material of the reinforcement that holds the ring. Calculations for this system have been performed using the boundary condition $\psi_P = 0$ on the ring surface. In a pulse field this corresponds to the condition of a pronounced skin effect. With a greater ratio of radii R_e/R_0 and the chosen value $R_0/h = 0.75$, the configuration of the left part of the equilibrium shape and the d_0/h ratio remain the same as in the system in Fig. 3. For the given module we have constructed configurations of a balanced boundary in the presence of shields having different radius R_S and different lengths g, have calculated magnetic field energy W_2, total radial force $\mathbf{F}_r$, reinforcement mass

$$M_2 = \gamma F_r R_S, \sigma_M, \qquad (17)$$

and have found the virial coefficient value for one element

$$\theta_2 = \frac{W_2}{R_S F_r}. \qquad (18)$$

The module in the example shown in Fig. 4 is balanced if $R_S = 3.2h$, $c = 0.18h$, $g = 0.05h$. Small variations of the given dimensions do not greatly affect the numerical value of energy and mass. They take on values $W_2 \sim 4.3W_0$ and $M_2 \sim 0.18M_0$. Reinforcement mass in the second type of the magnetic system is considerably smaller than in the first one. This is due to the fact that, even in case of a small cross-section of a short-circuited shield, its presence allows for constructing a boundary with the required boundary conditions (after appropriate selection of radius R_S). The virial coefficient for the module of the second type in this example takes on a much higher value than in the first one: $\theta_2 \sim 23.8$.

3. Construction of the magnetic system end parts

Rational construction of the end part is important because it ensures overall equilibrium of the magnetic system. At the same time, a significant part of the magnetic field energy and magnetic field mass can be concentrated in this region. The end part configuration is shown in Fig. 5. It is a combination of same-type elements. Each n-th element consists of a longitudinal and a transverse module with numbers n' and n''. Fig. 5 shows an example of a system with three such elements. The longitudinal and transverse modules of each element are separated by narrow gaps. These gaps virtually does not affect the field the force lines of which pass round the module boundaries. Each longitudinal module is characterized by inner radius R_n and outer radius R'_n. The end part boundary should be plane Y that divides the extreme module from a system of alternating transverse modules with number 0 into two equal parts. A half of the extreme module can be included into the end element. The poloidal field flux function on the given boundary can be taken equal to zero.

Distances between modules of adjacent elements, form of end sections and configuration of „rounded" boundaries at the junction of longitudinal and transverse modules of each element must be calculated so that the above-mentioned conditions of constancy of flux function ψ_i and the $B_p r$ product are met on the boundaries.

The first step in construction of a balanced end part of the system is calculation of the inner radius of the first longitudinal module R_1 and construction of a configuration of the region between the extreme element of the sequence of transverse modules and transverse module I'' (Fig. 5). Then we will proceed from the assumption that the radial size of these modules is much greater than the width of the gap between them d_1. Due to this, the values of poloidal field density B_P at points m_0 and n_1 having identical radial coordinates r in the middle of the gap d_1 can be

considered as equal. Parameter $G = B_p r$ at both points takes on the equal value $G_0 = 2\psi_0/d_0$. A difference of poloidal field flux functions at the given points can be represented as $\psi_0 - \psi_1 = B_p(M_0)rd_1 = G_0 d_1 = 2\psi_0 d_1/d_0$. The flux function at point a on the boundary of the longitudinal module I', located in the region where the poloidal field is virtually homogeneous, takes on the value $\psi_1 = -(1/2)B_1 R_1^2 = -(1/2)G_0 R_1 = -\psi_0 R_1/d_0$. It is taken into account that magnetic field vector $\mathbf{B}_1$ in the specified region has a different direction than vector $\mathbf{B}_0$, while parameter G_0 retains the same values as in the adjacent element. Expressions for the inner radius of longitudinal module I' and flux function ψ_1 follows from the given equations: $R_1 = 2d_1 - d_0$, $\psi_1 = \psi_0(1 - 2d_1/d_0)$. The value of gap d_1 is varied during construction of a boundary in the iteration process. Taking the determined value of d_1 and the corresponding values of radius R_1 and flux function ψ_1, we generate a shape on whose boundary the second boundary condition $R_1 B_1 = G_0$ is met, along with condition $\psi = const = \psi_1$. Fig. 5 shows the result of such construction. For the found values $d_0/h = 0.42$, $d_1/h = 0.49$, $R_{i,1}/h = 0.56$, the flux function at the boundary of the first module and flux density in the gap take on values $\psi_1 = -1.33\psi_0$, $B_1 = -8.5\psi_0/h^2$.

Cylindrical and flat thin-walled short-circuited shields S_n, in addition to longitudinal and transverse modules, are located in the end part. If the shields are absent, condition (4) cannot be met on the entire boundary of the gap between the adjacent modules. Indeed, the values of flux density at points m_n and n_{n+1}, located at the same distance from the axis and lying on the boundaries of the adjacent transverse modules with numbers n and $n + 1$, are equal. At the same time, the values of the $B_p r$ products are also equal on these parts of the boundaries. However, with equal flux densities at points e_n and f_{n+1}, located at the boundaries of the adjacent longitudinal modules with numbers n and $n + 1$, the values of the given product at these points are different, since the said points are at different distances R'_n and R_{n+1} from the axis. Consequently, a system must be created with differing values of flux densities at the boundaries of the adjacent longitudinal modules. To do so, short-circuited thin-walled cylinders (shields) S_n were placed between the specified modules. They are shown by the heavy lines in Fig. 5. Calculations of the magnetic system end part were performed on the assumption that the flux function of the poloidal field at the boundaries of all shields is constant and takes on value $\psi_p = 0$. Magnetic flux passes round each module. Thereat, the flux function of the poloidal field and parameter G_n are determined by the following expressions:

$$\psi_n = \frac{G_n}{2R_n}\left[R_n^2 - R_{S,n-1}^2\right] = \frac{G_n}{2R'_n}\left[R_{S,n}^2 - R'^2_n\right], \qquad (19)$$

where R_n — inner radius, R'_n — outer radius of the longitudinal module, $R_{S,n-1}, R_{S,n}$ — radii of the shields between which the given module is located. The ratios between the radii of the adjacent modules and shield radii
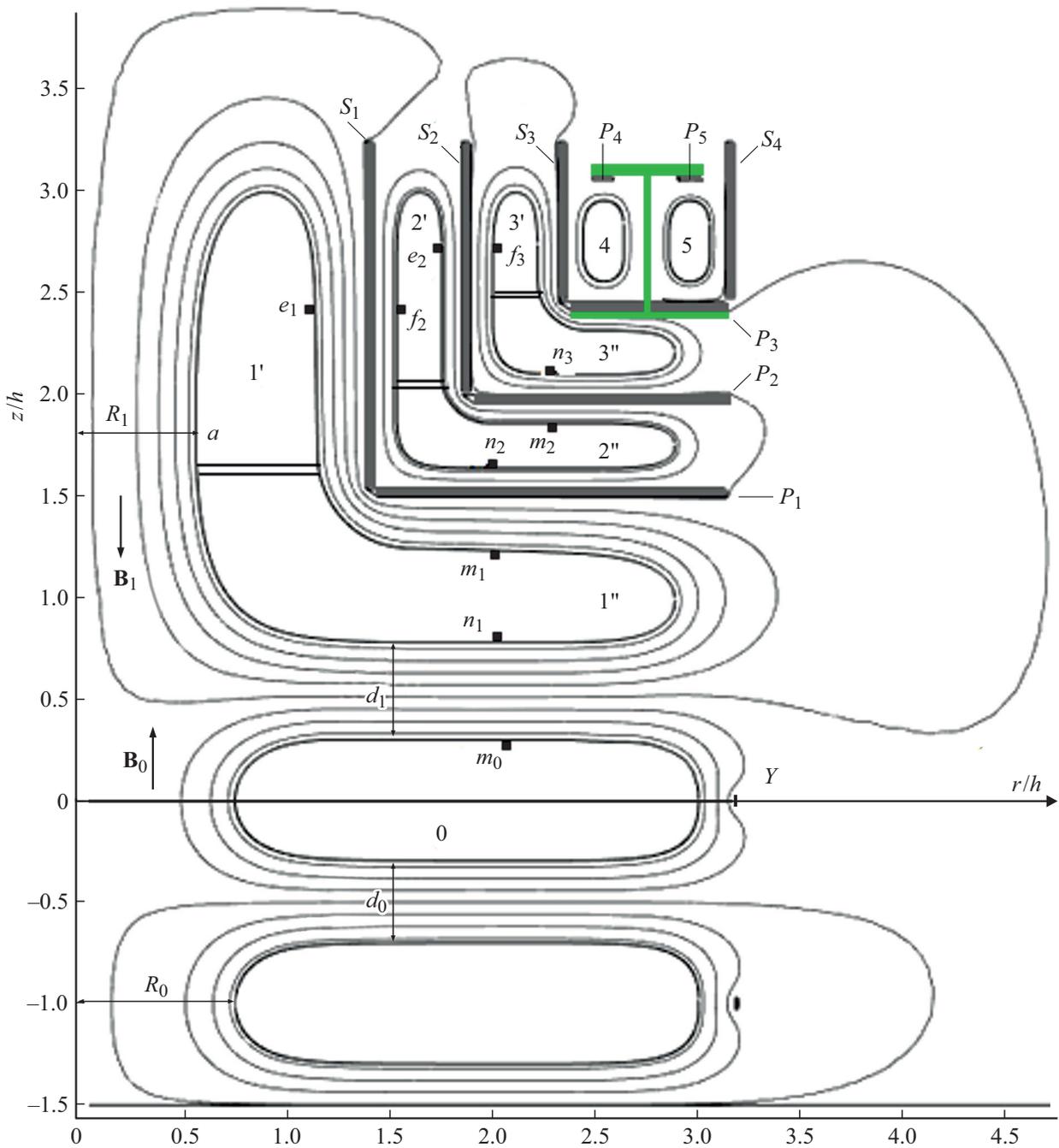
Figure 5. End part of a finite-length magnetic system with a combination of longitudinal and transverse modules and the adjoining part with a sequence of transverse modules.

must match the conditions of existence of configurations where the equilibrium conditions are met at the whole boundary of each longitudinal module, including its end part. In the considered example of a system composed of three two-module elements, given the chosen value of radius of the first longitudinal module $R_1 = 0.56h$, the outer radius of this module R'_1 and shield radius $R_{S,1}$ are determined by the above-mentioned ratios for a balanced thin-walled winding in a shield: $R'_1 = 2.12R_1 = 1.19h$, $R_{S,1} = 2.57R_1 = 1.44h$. The next longitudinal module is

located between two shields with radii $R_{S,1}$ and $R_{S,2}$. The longitudinal modules are examples of equilibrium shapes located between two coaxial shields — the inner and outer ones (Fig. 2, a). With the given value for the ratio of inner radius of n-th winding to radius of inner shield $R_n/R_{S,n-1}$, a configuration of the module with a constant value of the flux function and the $B_p r$ product can be constructed only with quite a well-defined value for the ratios of inner, outer radii of the module and the radius of the external shield $R_{S,n}$ to the radius of the internal shield $R_{S,n-1}$. The values of

these ratios are given in Fig. 2, *b*. Thicknesses of the second and third modules in the considered example in the first approximation are taken equal, while gaps between these modules and shields are taken equal to half the module width. These dimension ratios take place in a plane field. Their selection in this case is due to the fact that the gap thicknesses are small as compared to the inner radii of the said modules. This selection was used as the first approximation. Then an updated construction of the module boundaries using the iteration method is performed.

Axial forces in the system end part must be balanced. The configuration of the longitudinal modules satisfies this condition, while equilibrium of the shields is maintained using additional short-circuited thin-walled plane conductors P_n located between the transverse modules. Arrangement of these conductors makes it possible to avoid an axial force acting on the cylindrical shields, but a small axial force is generated and acts on the plane part of conductor P_n and its edge part (Fig. 6).

The said force can be balanced by magnetic pressure of the field in the gap between the transverse module and the said conductor. This can be achieved through appropriate selection of a value for the flux function of the poloidal field at the module boundary. Together with the cylindrical shields, the plane conductors break the computational region into autonomous fragments with a weak magnetic coupling between them. The signs of the flux function at the boundaries of the adjacent modules and the values of product $B_p r = G_n = $ const are different. „Rounded" areas of the boundaries at junctions of longitudinal and transverse modules are constructed in each fragment by the iteration method, condition (4) being maintained on the same areas. Cylindrical shields S_k in the system construction in the above-mentioned way are not balanced and must be held by reinforcements T_k, thickness of which are determined by the permissible value of mechanical stress determined by the difference of magnetic pressure on both shield sides. Lengths of cylindrical shields and, consequently, masses of

Figure 7. Angular element of the end part of the magnetic system with shields S_k, plane rings P_k and reinforcements T_k.

Figure 6. Fragment of the magnetic system end part located between the second and third modules. The arrows show the directions of the forces acting on plane conductor P_2. $\mathbf{F}_{r,2}$ — force acting on the cylindrical shield S_2 and transmitted by reinforcements T_2.

reinforcements can be sufficiently small in case of a rational selection of modules configuration. In an idealized system we can disregard the mass of the plane conductors released from integral axial forces. With such an assumption, only the mass of the reinforcements, which hold the cylindrical shields, is included in calculation of the virial coefficient for the end parts. The energy and mass of the end part also includes the energy and mass of a half of the extreme one from the above-mentioned system of transverse modules marked with 0 in Fig. 5.

The radial boundaries of transverse modules *1″*, *2″*, *3″* shown in Fig. 5 are balanced by selecting their configuration. Another element of the end part is a fragment that includes two short longitudinal modules *4* and *5*, short-circuited cylindrical shields S_3 and S_4, plane short-circuited conductors $P_3 - P_5$ (Fig. 7). Trial calculations are performed to choose an arrangement of these conductors which allows for construction (by the iteration method) of modules *4* and *5* on whose boundary the boundary conditions (3) and (5) are met. Cylindrical shields S_3 and S_4 and plane short-circuited conductors $P_3 - P_5$ are exposed to axial electromagnetic forces. These forces are perceived by a dielectric body consisting of two flat disks and connecting ring K. The upper disk receives axial forces $\mathbf{F}_4$ and $\mathbf{F}_5$ acting on conductors P_4 and P_5. The resultant of these forces is applied to the ring top and is directed along the z axis in the positive direction. The ring bottom is exposed to force $\mathbf{F}_6$ acting on conductor P_3 and the lower disk. The flux function at the boundary of the third module $\psi_3 = -0.84\psi_0$ in the considered example was calculated so that this force is in the negative direction and is numerically equal to sum $F_4 + F_5$. Thus, the whole set of the conductors shown in Fig. 7 is balanced in the axial direction. Tension stress originates in ring K with cross-sectional area S. Its absolute value in case of uniaxial tension is $|\sigma_z| = \sigma_M = F_6/S$. It determines the ring cross-section area. The radial forces acting on flat disks P_3, P_4, P_5 are negligible. Disregarding

Table 1. Normalized values of forces acting on the shields and the products of forces by shield radii

Shield number	0	1	2	3	4
$(\mu_0 h^2/4\pi\psi_0^2)F_{r,k}$	0.19	2.20	0.73	3.08	0.78
$(\mu_0 h/4\pi\psi_0^2)R_r F_{r,k}$	3.20	1.39	1.92	7.07	2.51

Table 2. Virial coefficient for a system with a different number of transverse modules

N (number of modules)	1	10	20	30	40
θ_Σ (the first module type)	2.35	3.81	4.75	5.35	5.76
θ_Σ (the second module type)	2.35	4.32	6.09	7.51	8.83

the mass of these bodies, mass of the dielectric body can be taken equal to the mass of ring K:

$$M_K \approx \gamma S l_K = \frac{\gamma F_6 l_K}{\sigma_M}, \qquad (20)$$

where l_K is length of ring K.

Subsequent calculation was performed for a system where all the short-circuited conductors, exposed to radial forces, are held by dielectric reinforcements. Dielectric material density γ is taken equal for all the cylindrical reinforcements of the system and for ring K. The reinforcements are shown in some figures (Fig. $1-4, 6, 7$). When calculating the mass of the loaded elements in the end part of magnet M_3, we can neglect the mass of the conductors if their thickness is small as compared to thickness of the dielectric reinforcements, and use formula (17):

$$M_3 = \frac{\gamma}{\sigma_M}\left(\sum R_k F_{r,k} + F_6 l_K\right), \qquad (21)$$

where R_k — radii of all thin-walled cylindrical shields, $F_{r,k}$ — radial forces acting on them.

The poloidal and azimuthal fields of the magnetic system end part were calculated using the Comsol Multiphysics program, the energy of the poloidal and azimuthal fields of the end part W_3 and the forces included in formula (21) were found. As in the calculation of system A, boundary conditions $\psi_0 = 1$ and $h = 1$ were adopted. The results of calculation of dimensionless forces $(\mu_0 h^2/4\pi\psi_0^2)F_{r,k}$ are given in Table 1.

The typical parameters for the holding system of angular modules *4* and *5* are $(\mu_0 h^2/4\pi\psi_0^2)F_6 = 0.28$, $l_K/h = 0.6$. This data was used to calculate the energy, mass and virial parameter of the magnetic system end part:

$$(\mu_0 h/4\pi\psi_0^2)W_3 \sim 38.2, \quad (\sigma_M\mu_0 h/\gamma 4\pi\psi_0^2)M_3 \sim 16.2,$$

$$\theta_3 = \frac{\gamma W_3}{\sigma_M M_3} \sim 2.35. \qquad (22)$$

The virial coefficient for a complete system, comprising N alternating transverse modules of the first or second type, can be calculated using the formula

$$\theta_\Sigma = \frac{\gamma[(N-1)W_{1,2} + 2W_3]}{\sigma_M[(N-1)M_{1,2} + 2M_3]}. \qquad (23)$$

The number of transverse modules in this formula was reduced by one since the energy and mass of one of them

are taken into account in the calculation of the end parts. The minimum value of this parameter, θ_Σ equal to θ_3, occurs at $N = 1$. The limit values of virial coefficients $\theta_\Sigma = \theta_1 \sim 8.06$ and $\theta_2 \sim 23.8$ are achieved in a system of unlimited length ($N \gg 1$) for the two above-mentioned kinds of transverse modules.

The data of Table 2 shows that values of θ_Σ, considerably greater than unity, for the chosen dimensions of the magnetic system elements are achieved when number N is approximately several tens.

Conclusion

Mass of a magnetic system with conductors released from electromagnetic forces is chiefly determined not by the winding but by the elements exposed to the action of these forces. Such elements are reinforcements that hold the unbalanced parts of the windings and additional short-circuited shields. The possibility to reduce the mass of these elements has been considered within the framework of a perfect system with a thin force-free winding. The performed construction and calculations have demonstrated the efficiency of using a system with many alternating modules in combination with multi-module end parts of a special configuration. Application of a combination of longitudinal and transverse modules makes it possible to minimize the mass of elements loaded by electromagnetic forces. This can result in a considerable increase of values of the virial coefficient that characterizes the energy to mass ratio. The described methods for construction of equilibrium shapes can be used in subsequent optimization of similar magnetic systems. A key aspect in their construction is the use of a combination of longitudinal and transverse modules. Along with that, the suggested configurations provide a basis for construction of magnetic systems with quasi-force-free windings and calculation of the virial coefficient taking into account the mass of the balanced conductors.

Appendix

Construction of a free boundary by the iteration method

The iteration method is used to solve a problem with two boundary conditions (2), (4), specified at the boundary with an unknown configuration (the free boundary problem [19]). Radii-vectors of boundary points can be conveniently presented as complex numbers: $p(s) = z(s) + ir(s)$, where s

is the parameter — arc length counted from the beginning of the free boundary with specified coordinate $p(0) = p_0$. The magnetic field vector for poloidal field $\mathbf{B}(s)$ at this point is also written in the complex form. The iteration process consists of two stages.

Stage 1. Each iteration step includes a calculation of the magnetostatic problem with the specified boundary condition (2) through solving of an integral equation of the first kind. The boundary is assigned at the first step by an initial approximation, the boundary calculated at the previous step is used at each subsequent step. Magnetic field vector $\mathbf{B}_1(s) = B_1(s)\exp(i\alpha_1)$ is directed along a tangent line towards the conductor boundary, where α_1 is the tangle line direction angle. Then, according to the equilibrium condition, we adopt $|B_\varphi(s)| = B_1(s)$ and calculate constant C_2 by averaging the function $r|B_\varphi(s)|$ at a boundary with length l:

$$C_2 = \frac{1}{l}\int_l r|B_\varphi(s)|dl(s).$$

Stage 2. The integral equation of the second kind is solved to calculate the magnetostatic field with boundary condition (4), where constant C_2 was determined at the first stage. The magnetic field vector at the boundary takes on a new value $\mathbf{B}_2 = B_2\exp(i\alpha_2)$ and changes its direction by angle $\Delta\alpha = \alpha_2 - \alpha_1$

A change of the angle means a violation of boundary condition (2), according to which the magnetic field vector must be directed along a tangent line towards the boundary. To meet condition (2), we choose a new value for the angle of tangent line slope at each point of boundary $\alpha' = \alpha + \lambda\Delta\alpha$, where λ is the iteration parameter that accelerates process convergence: $1 < \lambda < 2$ A new coordinate for a free boundary node with number $k + 1$ at the given value of the angle of tangent line slope towards boundary $dp/ds = \exp(i\alpha'(s))$ can be calculated using the trapezoid formula: $p_{k+1} = p_k + h_k\exp[0.5i(\alpha'_k + \alpha'_{k+1})]$, $k = 0, \ldots, N - 1$, where N is number of free boundary elements, α'_k, α'_{k+1} is tangent line slope angle at the initial and final point of each element, h_k is its length. h_k was chosen so that the node points displaced in the given direction (usually in parallel to one of the coordinate axes).

The iteration process is continued until the following condition is met with the specified accuracy: $\alpha_2 - \alpha_1 = 0$. The examples of plane problem, which allow a comparison with an analytical solution, have confirmed the convergence of the iteration process on the basis of on an initial approximation which is far from the final one [20].

Funding

Conflict of interest

The authors declare that they have no conflict of interest.

References

[1] E.N. Parker. Phys. Rev., **109** (5), 1440 (1958).

[2] K. Longmire. *Fizika plazmy* (Atomizdat, M., 1966), 341 p. (in Russian).

[3] V.D. Shafranov. In: *Voprosy teorii plazmy,* ed. by M.A. Leontovich (Gosatomizdat, M., 1963), p. 92 (in Russian).

[4] B.A. Larionov, F.M. Spevakova, A.M. Stolov, E.A. Azizov. In: *Fizika i tekhnika moschnykh impulsnykh sistem,* ed. by E.P. Velikhov (Energoatomizdat, M., 1987), p. 66 (in Russian).

[5] Y.M. Eyssa, R.W. Boom. IEEE Trans. Magnet., **MAG.17** (1), 460 (1981).

[6] W. Hassenzahl. IEEE Trans. Magnet., **MAG.25** (2), 1854 (1989).

[7] M.A. Hilal, O. Arici, M. Cuban. IEEE Trans. Magnet., **MAG.21** (2), 1044 (1985).

[8] F.C. Moon. J. Appl. Phys., **53** (12), 9112 (1982).

[9] S. Nomura, T. Osaki, J. Kondoh, H. Tsutsui, S. Tsuji-Lio, Y. Sato, R. Shimada. IEEE Trans. Appl. Superconductivity, **9** (2), 354 (1999).

[10] S. Nomura, H. Tsutsui, N. Watanabe, C. Suzuki, S. Kajita, Y. Ohata, T. Takaku, E. Koizumi, S. Tsuji-Lio, R. Shimada. IEEE Trans. Appl. Superconductivity, **13** (2), 1852 (2003).

[11] S. Nomura, H. Tsutsui. **27** (4), 5700106 (2017).

[12] H. Kamada, A. Ninomiya, S. Nomura, T. Yagai, T. Nakamura. IEEE Trans. Appl. Superconductivity, **30** (4), 4600905 (2021).

[13] G.A. Shneerson, M.I. Dolotenko, S.I. Krivosheev. *Strong and Superstrong Pulsed Magnetic Fields Generation* (Berlin, De Gruyter, 2014), p. 429.

[14] G.A. Shneerson, A.P. Nenashev., A.A. Parfentiev., I.A. Vecherov., S.A. Shimanskiy. IEEE Transactions on Plasma Science. **46** (9), 3209 (2018).

[15] M.E. Gurevitch. *Teoriya struy idealnoy zhidkosti* (Nauka, M., 1979) (in Russian)

[16] A.B. Novgorodtsev, F.R. Fatkhiyev. Radiotekhnika i elektronika. (5), 874 (1982) (in Russian).

[17] G.A. Shneerson. *Fields and Transients in Superhigh Pulse Current Devices* (Nuova Science, NY, 1997), p. 561.

[18] E.L. Amromin, G.N. Kaporskaya, A.B. Novgorodtsev, S.L. Shishigin, G.A. Shneerson. Elektrichestvo, (3), 40 (1989) (in Russian).

[19] S.L. Shishigin. Elektrichestvo. (9), 51 (2008) (in Russian).

[20] G.A. Shneerson, A.A. Parfentyev, V.V. Titkov, S.I. Krivosheyev, A.D. Lagutkina, A.S. Nemov, A.P. Nenashev, S.A. Shimansky. Pisma v ZhTF, (11), 40 (2021) (in Russian).